https://doi.org/10.48048/tis.2025.9010

Antimalarial Potential of Ostruthin Isolated from *Luvunga sarmentosa* Root and Stem: *In Vitro* and *In Silico* Studies

Waqar Ahmad[1], Firman Wicaksana[2], Hilkatul Ilmi[1,3], Lidya Tumewu[3], Muhammad Faturrahman[4], Peggy Ignatia Winarko[4], Cindi Dia Rakhmawati[4], Suciati Suciati[3,5], Achmad Fuad Hafid[3,5] and Aty Widyawaruyanti[3,5,*]

[1]*Doctoral Program of Faculty of Pharmacy, Universitas Airlangga, Surabaya, Indonesia*
[2]*Master Program of Faculty of Pharmacy, Universitas Airlangga, Surabaya, Indonesia*
[3]*Natural Product Medicine Research and Development, Institute of Tropical Disease, Universitas Airlangga, Surabaya, Indonesia*
[4]*Undergraduate Program of Faculty of Pharmacy, Universitas Airlangga, Surabaya, Indonesia*
[5]*Department of Pharmaceutical Sciences, Faculty of Pharmacy, Universitas Airlangga, Surabaya, Indonesia*

([*]Corresponding author's e-mail: aty-w@ff.unair.ac.id)

Received: 16 September 2024, Revised: 20 October 2024, Accepted: 6 November 2024, Published: 30 December 2024

Abstract

The high morbidity and mortality due to malaria infection worldwide led to the demand for new antimalarial drug development, one of which is utilizing herbal medicines as a new alternative to malaria treatment. This study aims to isolate and identify antimalarial compounds from *Luvunga sarmentosa* root and stem by bioassay-guided isolation approach. *Luvunga sarmentosa* root and stem were extracted, fractionated and purified to obtain an antimalarial compound. Compound identification was conducted based on ^{1}H, ^{13}C and 2D NMR. The LDH assay was used to test the antimalarial activity against *Plasmodium falciparum*. A molecular docking study was performed on *Pf*DHODH (PD-ID: 1TV5) and *Pf*LDH (PD-ID: 1LDG) using Autodock tools. The bioassay-guided isolation obtained a coumarin compound identified as ostruthin (6-geranyl-7-hydroxycoumarin) as antimalarial isolated from *L. sarmentosa* root and stem extract. Ostruthin exhibited antimalarial activity with an IC_{50} value of 2.65 ± 0.07 µg/mL against *P. falciparum*. The molecular docking results showed that ostruthin was predicted as a potential *Pf*DHODH and *Pf*LDH inhibitor based on their binding affinity which are −9.94 ± 0.11 and −8.84 ± 0.11 kcal/mol, respectively, and their interaction with receptor's amino acids. Ostruthin isolated from the root and stem of *L. sarmentosa* is active as an antimalarial, and further research, such as *in vivo* studies and clinical trials, is needed to develop this compound as a drug.

Keywords: Antimalarial, LDH assay, Coumarin, *Luvunga sarmentosa*, Molecular docking, *Pf*DHODH, *Pf*LDH

Introduction

Morbidity and mortality due to malaria infection in subtropical and tropical areas are still high, making this disease a major health problem worldwide. At present, 249 million positive malaria cases in 84 malaria-endemic countries and 608,000 deaths have been reported [1]. Malaria cases in Indonesia exceeded 369,000 in 2023, with increased cases in regions such as Gorontalo, East Nusa Tenggara and Papua [2].

Of the 5 species that cause human malaria, *Plasmodium falciparum* and *Plasmodium vivax* are most commonly found to infect humans, with the highest rates of complications and mortality. Around 38.32 % of people in Indonesia are infected with *Plasmodium falciparum* and 47.93 % with *Plasmodium vivax*. Meanwhile, around 90 % of cases in Sudan are due to *P. falciparum*, associated with a higher case fatality rate than *P. vivax* [1,2]. Both species also have confirmed resistance against most currently available antimalarial agents. Artemisinin and its derivatives have been widely implicated in combating drug-resistant

Plasmodium in endemic regions. Still, the appearance of artemisinin resistance, first in Cambodia in 2007 [3] and later its rapid spread to the Southeast Asian region has threatened all the previous success incurred by malaria control strategies. Therefore, it is necessary to develop new antimalarials, one of which is utilizing herbal medicines as a new alternative to treat malaria.

In searching for and developing antimalarial drugs, herbal plants are a potential source because they have many pharmacological and minimal adverse effects [4]. Efforts to discover drug compounds from plants can be made by isolating active antimalarial compounds using bioassay-guided isolation. One plant widely used in traditional medicine is the genus *Luvunga*. The stem decoction of *Luvunga scandens* is traditionally used to treat malaria in Indonesia and China [5,6]. *In vitro* studies show that dichloromethane extracts of *L. scandens* leaves (LS-L-D) and stem (LS-S-D) inhibit *P. falciparum* with IC_{50} values of 6.61 ± 0.04 and 5.38 ± 0.01 µg/mL, respectively. Both extracts are nontoxic against the HepG2 cell line [7]. Another species of the genus *Luvunga*, is also widely used in traditional medicine including *Luvunga sarmentosa*.

Luvunga sarmentosa, commonly known as saluang belum, has grown and spread in the tropical forests of Kalimantan. Phytochemical screening showed the presence of alkaloids, polyphenols and terpenoids [8,9]. Potirucallane triterpenoids named *luvungins* A-G, 1α-acetoxyluvungin A, coumarins ostruthin and 8-geranyl-7-hydroxycoumarin, and triterpenes, friedelin, flindissone, melianone, niloticin and limonin were compounds isolated from *L. sarmentosa*. Traditionally, the Dayak tribe has used this plant to treat aphrodisiacs and fever. This is accomplished by boiling with water and consumed once a day [10,11]. In this study, *L. sarmentosa* has been chosen as a candidate for antimalarial based on the ethnopharmacological approach, namely this plant is used to treat fever associated with malaria. Furthermore, a chemotaxonomic approach was adopted referring to *L. scandens* which is known to be active as antimalarial. Plants belonging to 1 genus tend to have similar chemical components, therefore further research was taken to isolate antimalarial active compounds from root and stem of *L. sarmentosa*. In addition, the antimalarial activity of this plant has not been reported. Hopefully, this research will yield an effective and safe compound for malarial treatment. Moreover, the mechanism of the isolated compound with the *Pf*DHODH and *Pf*LDH enzyme was also evaluated using a molecular docking technique.

Materials and methods

Plant material

The roots, stems and leaves of *L. sarmentosa* were collected in August 2019 from traditional healers in the Center of Kalimantan, Indonesia. A licensed botanist at Purwodadi Botanical Garden Growth Conservation Center, East Java, Indonesia (1048/IPH.06/HM/IX /2019) confirmed the identity of the plant material, where voucher specimens (collection numbers: LSa-R, LSa-S, and LSa-L) were deposited.

Extraction and isolation

The plant materials of *L. sarmentosa* (root, stem and leaves) were dried at room temperature (± 27 °C) without exposure to direct sunlight and mechanically powdered. The maceration technique conducted successive maceration on dried powder (250 g) with n-hexane, dichloromethane and methanol. The extract was filtered and concentrated with a rotary evaporator and then dried in an oven temperature of 40 ℃ to obtain a dry extract. The extraction process resulted in 9 extracts namely: *Luvunga sarmentosa*-root hexane extract (LSa-R-H), dichloromethane extract (LSa-R-D), methanol extract (LSa-R-M), *Luvunga sarmentosa*-stem hexane extract (LSa-S-H), dichloromethane extract (LSa-S-D), methanol extract (LSa-S-M), *Luvunga sarmentosa*-leaves hexane extract (LSa-L-H), dichloromethane extract (LSa-L-D) and methanol extract (LSa-L-M). The extracts were preserved in glass sample bottles and kept at 4 °C for further use.

After the initial antimalarial screening and determining the IC_{50} value, LSa-R-D exhibited the strongest activity and chose to separate further. The LSa-R-D (2 g) was fractionated under vacuum liquid chromatography (VLC) with hexane-EtOAc and chloroform-methanol solvent gradient (100:0 - 0:100) and produced 15 fractions (F1 - F15). Only 8 fractions (F6 - F13) showed more than 50 % inhibition on antimalarial screening. Subsequently, the IC_{50} value of the active fraction is determined, F7 showed the strongest activity and was carried out to the next separation. The F7 (320 mg) was separated using Colum

Chromatography with acetonitrile-water (7.5:2.5 v/v) to give 10 fractions (F7.1 - F7.10). Fraction (F7.8) was identified as compound (1).

The chemical structure of compound (1) was determined using NMR-JEOL ECS 400 with $CdCl_3$ as the solvent, based on proton signals in the ^1H NMR spectrum, carbon signals in the ^{13}C NMR spectrum, heteronuclear multiple bond correlation (HMBC), heteronuclear multiple quantum correlations (HMQC) and compared to the reference [15].

Besides LSa-R-D, LSa-S-D showed strong antimalarial activity as well. The extraction was conducted for *L. sarmentosa* stem using different methods as follows: *L. sarmentosa* stem powder (500 g) was extracted with n-hexane (2 L) to remove the lipid section. Furthermore, the resulting residue was subjected to an acid-base process. The marc's precipitate of *L. sarmentosa* was alkalinized using ammonia (NH_4OH) solution (150 mL) to pH 11 for 1 h and added dichloromethane (3 L), left for 12 h. Furthermore, filtered and concentrated using a rotary evaporator at 40 °C. The dichloromethane extract (1.932 g) was continued with an acid-base process using NH_4OH pH 11 and 5 % HCl pH 2. This process obtained the dichloromethane fraction (DF).

DF (339.9 mg) was separated using a silica gel column with gradient elution of chloroform-methanol (95 - 5 % v/v) with an increasing amount of methanol to 100 % and obtained 12 fractions (SF1-12). Fraction 3 (SF3, 128.6 mg) was separated using preparative TLC RP-18 (20×20 cm^2) with Acetonitrile:Water (2:1 v/v) as mobile phase, generated 7 subfractions (SF3.1 - 3.7). SF3.2 was purified using semipreparative-HPLC utilizing a solvent composition of Acetonitrile:Water (2:1 v/v) and afforded compound (1) (6.2 mg) from SF3.2.

In vitro culture of malaria parasite

P. falciparum laboratory strain 3D7 (chloroquine-sensitive) and strain Dd2 (chloroquine, pyrimethamine and mefloquine-resistant) were maintained in the Natural Product Research Medicine and Development (NPMRD), Institute of Tropical Disease (ITD), Universitas Airlangga. Parasites were thawed and grown in Human Red Blood Cells (RBC) with blood type O at 37 °C controlled conditions (5 % oxygen, 5 % carbon dioxide and 90 % nitrogen), in RPMI-1640 tissue culture medium supplemented with 50 µg/mL hypoxanthine, 25 mM HEPES, 0.3 g/L L-glutamine, 11 mM glucose, 25 mM $NaHCO_3$, 2.5 µg/mL gentamicin and 0.5 % w/v Albumax II. Sorbitol treatment synchronizes the parasite culture to obtain a homogenous ring stage [13].

Antimalarial activity and determination of IC_{50} values

The sample's antimalarial activity (9 extracts of LSa) was tested against *P. falciparum* 3D7 strains using the LDH assay method based on Wang *et al.* [14]. Meanwhile, the fractions of DF were tested against *P. falciparum* strain Dd2. For the initial screening of antimalarials, a single concentration of 5 µg/mL of sample dissolved in DMSO. The IC_{50} value was determined for samples that showed a more than 50 % inhibition of malaria parasites. Eight concentrations (2-fold) of each sample and standard drug (chloroquine) were added to the 96-well plates. The sample and standard drug concentration ranges were 50 to 0.01 and 10 to 0.001 µg/mL, respectively. All the treatments were performed in triplicates. Then, 100 µL of parasitized blood was added to each well plate. The plates were incubated at 37 °C in an environment of 5 % oxygen, 5 % carbon dioxide and 90 % nitrogen for 72 h. After the incubation period, the harvest plate was performed and stored at −30 °C. Subsequently, 90 µL of the prepared substrate was put into each well plate, covered with aluminum foil, and placed in a flatbed shaker at 650 rpm (room temperature) for 30 min. The absorbance of each well was measured using the multiscan sky-high microplate spectrophotometer (Thermo Fisher Scientific) at a wavelength of 650 nm.

Finally, the IC_{50} values were calculated using GraphPad Prism (GraphPad Prism v.9 San Diego, California, USA). Based on the obtained IC_{50} values, the extracts were categorized into active (< 10 µg/mL), moderate (10 - 50 µg/mL) or inactive (> 100 µg/mL) classifications [16,17]. Isolated compound(s) were classified as potent (IC_{50} < 1 µM), promising (1 < IC_{50} < 20 µM), moderate (20 < IC_{50} < 100 µM) and inactive (IC_{50} > 200 µM) [18].

Molecular docking

Compound (1) has been integrated into both proteins such as *Pf*DHODH (PD-ID: 1TV5) and *Pf*LDH

(PD-ID: 1LDG). The torsional root and branches of the ligands were selected using Autodock tools 1.5.6, which accommodated all rotatable bonds except the amide bond. Moreover, the Kollman charges for each protein and Gasteiger-Marsili atomic charges for all ligands were assigned using Autodock tools 1.5.6. Next, the chemicals were positioned in the binding site using the Lamarckian genetic process from the AutoDock 4.2.6 software. A grid box with dimensions of *Pf*DHODH (32×34×40 $Å^3$) and *Pf*LDH (40×40×40 $Å^3$) was used to compute the atom-type maps. The grid boxes were spaced 0.375 A apart and centered in the cocrystallized ligand's binding pocket. We conducted 100 runs, evaluating a maximum of 2,500,000 energy values and starting with 150 conformers as beginning populations. The optimal binding mode of each molecule was chosen by considering the minimum computed free binding energy and the size of the protein cluster. The docking results were analyzed using Autodock tools and PyMol, and a validated molecular docking procedure was repeated 3 times. Consulting with the Banerjee *et al.* [19], the binding energy ≤ −5.0 kJ/mol was used as the criterion to judge the better binding ability of the molecule to the target.

Toxicity prediction

Prediction of Toxicity for ostruthin form *L. sarmentosa* was done by the Protox-III website (https://tox.charite.de/protox3) with the SMILES format and the results is illustrated using images by analyzing organ toxicity and toxicity endpoints such as hepatoxicity, immunotoxicity, mutagenicity, carcinogenicity and cytotoxicity [19]. These parameters were calculated and checked for compliance with their standard.

Results and discussion

Antimalarial activity of extract and fractions of *L. sarmentosa*

The dry powder of the root, stem and leaves of *L. sarmentosa* was extracted using different solvents' polarities, starting from n-hexane, dichloromethane and methanol to give 9 extracts. The methanol extracts had the highest yield (%) compared to n-hexane and dichloromethane in all plant parts. Then, these extracts were examined against *P. falciparum* 3D7. The results revealed that 4 extracts (LSa-R-H, LSa-R-D, LSa-S-D and LSa-L-D) were active as antimalarial with IC_{50} values of 7.32 ± 0.02, 2.14 ± 0.07, 2.85 ± 0.04 and 6.59 ± 0.02 µg/mL, respectively. In contrast, the remaining extracts were moderately active as antimalarial (**Table 1**). Of the 4 active extracts, LSa-R-D and LSa-S-D had relatively high antimalarial activity compared to the other extracts, they have similar IC_{50} values and there was no significant difference between them ($p > 0.05$). Based on the data, LSa-R-D and LSa-S-D were chosen as the priority for further isolation to obtain antimalarial active compounds following the bioassay-guided isolation approach. Therefore, further fractionation and isolation of compounds were conducted from both extracts.

Table 1 The percent of yield (%) and antimalarial activity of all extract from *L. sarmentosa* roots, stems and leaves against *P. falciparum* 3D7.

Part of plant	Code	Yield (% w/w)	IC_{50} (µg/mL)*
Root	LSa-R-H	1.09	7.32 ± 0.02
	LSa-R-D	1.83	2.14 ± 0.07
	LSa-R-M	5.19	25.06 ± 0.02
Stem	LSa-S-H	0.19	22.48 ± 0.04
	LSa-S-D	0.42	2.85 ± 0.04
	LSa-S-M	2.43	24.92 ± 0.06
Leaves	LSa-L-H	1.73	11.54 ± 0.03
	LSa-L-D	1.88	6.59 ± 0.02
	LSa-L-M	5.48	27.26 ± 0.04

*Mean ± SD of triplicate, LSa: *Luvunga sarmentosa*, R: Root, S: Stem, L: Leaves, H: Hexane, D: Dichloromethane, M: Methanol.

The LSa-R-D was fractionated to obtain 15 fractions (F1 - F15). Only 8 fractions (F6 - F13) showed more than 50 % inhibition on antimalarial screening at a 5 µg/mL concentration. Subsequently, the IC_{50} value of the active fraction is determined (**Figure 1**). According to the antimalarial criteria, all fractions are active as antimalarials, with IC_{50} values ranging from 2.65 ± 0.07 to 0.75 ± 0.02 µg/mL. The F7 exhibited the strongest activity, with an IC_{50} value of 0.75 ± 0.02 µg/mL. Statistical analysis shows that there is a significant difference in the IC_{50} value between F7 and all fractions ($p < 0.05$). Then, the F7 was separated to give 10 fractions. Fraction (F7.8) produces compound (1), forming yellow amorphous crystals. Compound (1) exhibited antimalarial activity with an IC_{50} value of 2.65 ± 0.07 µg/mL. The compound (1) antimalarial activity was not a significant difference ($p > 0.05$) to LSa-R-D but less than F7. The decreasing activity of stand-alone compounds might be due to the synergism activity of compounds contained in F7. Compound (1) has antimalarial activity lower than the positive control. However, compound (1) is still included as an active antimalarial substance due to its IC_{50} value of less than 10 µg/mL. This compound has the potential to be further studied. Therefore, further research is needed to improve its antimalarial activity, such as structural modification or use in combination with standard drugs or other compounds.

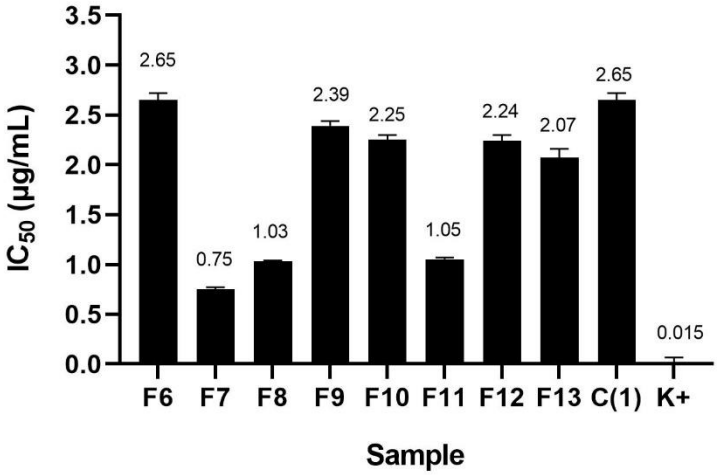

Figure 1 Antimalarial activity of LSa-R-D fractions, compound (1) and standard drug (K+) against *Plasmodium falciparum* 3D7. The data are represented as Mean ± SD of triplicate.

Meanwhile, the antimalarial activity of dichloromethane fraction (DF) dan SF3-8 of *L. sarmentosa* stem which resulted from extraction with the acid-base method was conducted against *P. falciparum* strain Dd2. The results showed that DF and SF3-8 exhibited antimalarial activity with IC_{50} values < 10 µg/mL (**Figure 2**). SF3 was chosen for further separation due to its sufficient amount compared to other active fractions. From the separation of SF3, compound (1) was obtained. The identification of compound (1) was conducted by comparison of ^{1}H and ^{13}C NMR spectrum of compound (1) from SF3, compound (1) from LSa-R-D F7.8 and reference data.

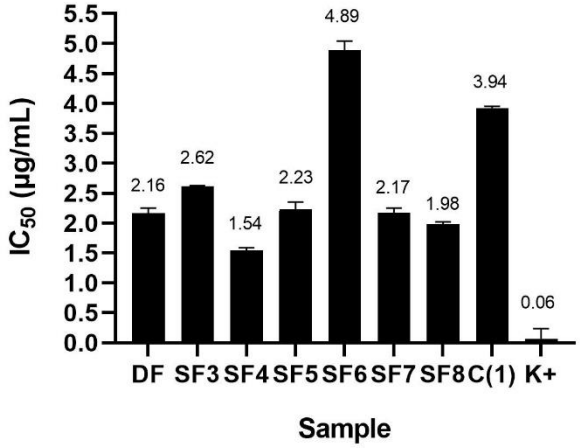

Figure 2 Antimalarial activity of DF and SF3 against *P. falciparum* Dd2. The data are represented as Mean ± SD of triplicate.

In this study, ostruthin was found in the roots and stems of *L. sarmentosa*. This compound was obtained using different isolation procedures. Ostruthin (coumarin group) is isolated from the stems using the acid-base extraction method. This compound is relatively stable to pH 11, so acid-base reactions can extract it [20]. Isolation of other active fractions from the root and stem of *L. sarmentosa* needs to be carried out to obtain other compounds that are also active as antimalarials.

Identification of compound (1)

Compound (1) was obtained as a yellow amorphous crystal. Identification was conducted based on ^{1}H, ^{13}C and 2D NMR, and comparison with reference data, to establish compound (1) as coumarin namely ostruthin (6-geranyl-7-hydroxycoumarin) with molecular formula $C_{19}H_{22}O_3$ [15]. The occurrence of the coumarin nucleus in the molecule could be deduced from the ^{1}H NMR spectrum (**Table 2**), which shows signals for H-3, H-4, H-5 and H-8. The AB-coupling between H-3 and H-4 was observed. The presence of geranyl side-chain was detected by a set of geranyl signals consisting of 3 methyl signals (CH_3-3', 7' and 8'), 2 methine signals (H-2', H-6') and 3 methylene signals (H-1', H-4' and H-5'). The HMBC correlation of H-1' with a quarternary carbon C-6, and H-5 correlates to C-1' indicating that C-1' was attached to C-6. The chemical structure of compound (1) is shown in **Figure 3**.

Table 2 ^{1}H (400 MHz) and ^{13}C (100 Hz) NMR data of compound (1) in $CdCl_3$ compared to the reference.

Position	Compound (1)		Reference
	δ_H ppm, *J* (Hz)	**δ_C ppm**	**δ_H ppm, *J* (Hz)**
1	-	-	-
2	-	162.7	-
3	6.23 (1H, d, *J* = 9.6 Hz)	112.1	6.24 (1H, d, *J* = 9.5 Hz)
4	7.65 (1H, d, *J* = 9.6 Hz)	144.5	7.65 (1H, d, *J* = 9.5 Hz)
5	7.19 (s)	128.3	7.20 (s)
6	-	126.0	-
7	-	158.8	-
8	7.05 (s)	103.2	7.01 (s)
9	-	154.1	-
10	-	112.2	-
1'	3.38 (2H, d, *J* = 7.2 Hz)	28.3	3.40 (2H, d, *J* = 7.2 Hz)

Position	Compound (1)		Reference
	δ_H ppm, *J* (Hz)	**δ_C ppm**	**δ_H ppm, *J* (Hz)**
2’	5.32 (1H, tq, *J* = 7.2, 1.2 Hz)	120.9	5.33 (1H, tq, *J* = 7.2, 1.2 Hz)
CH_3-3’	1.73 (3H, s)	16.2	1.74 (3H, d, *J* = 1.2 Hz)
3’	-	138.6	-
4’	2.10 (2H, m)	39.7	2.10 (2H, m)
5’	2.10 (2H, m)	26.5	2.10 (2H, m)
6’	5.09 (1H, tq, *J* = 6.8 Hz)	124.0	5.09 (1H, br.t, *J* = 6.8 Hz)
CH_3-7’	1.59 (3H, s)	17.8	1.60 (3H, br.s)
7’	-	131.9	-
CH_3-8’	1.68 (3H, s)	25.8	1.69 (3H, br.s)

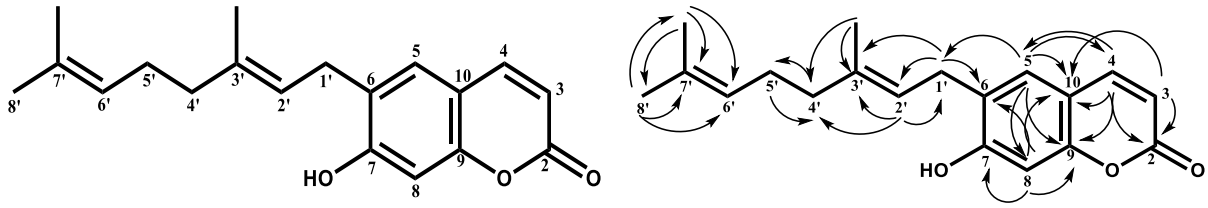

Figure 3 Chemical structure of compound (1): Ostruthin (6-geranyl-7-hydroxycoumarin) and the HMBC correlation of compound.

Molecular docking

Validating the docking procedure and its parameters using the redocking approach is necessary before docking with test molecules. The co-crystal ligands employed were FMN and NAI, which were successfully docked with the target proteins *Pf*DHODH and *Pf*LDH, respectively. The root mean square (RMSD) of the redocked findings was found to be less than 2 Å. This conclusion supports the validity of the utilized technique (**Figure 4**). The docking predictions validated that the ligand binds to its target close to its actual conformation, therefore confirming the dependability of the docking technique and parameters.

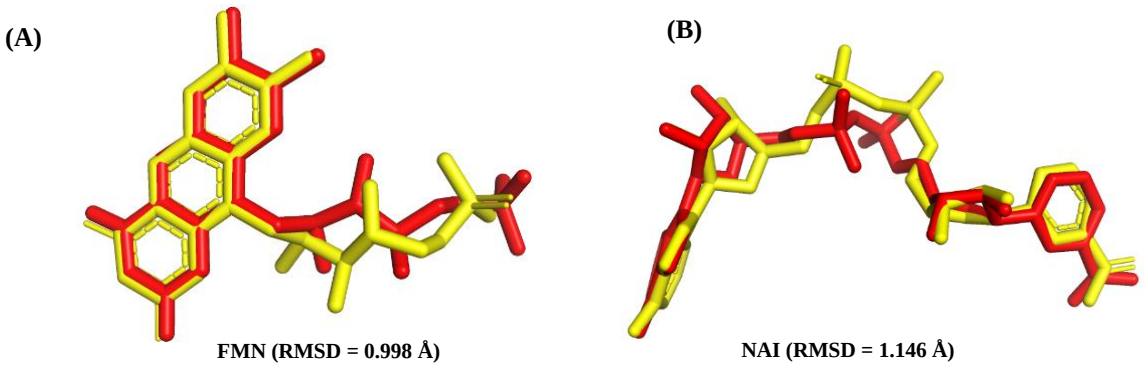

Figure 4 Validation of Molecular docking result. Original co-crystal position (yellow) and docked poses (red) at receptors PfDHODH (A) & PfLDH (B).

The binding affinity (kcal/mol) value of compound (1) for the *Pf*DHODH and *Pf*LDH proteins is detailed in **Table 3**. Compound (1) showed a higher binding affinity value for each protein when compared

to chloroquine. This result is evidenced by the presence of hydrogen bonds; compound (1) in *Pf*DHODH interacts with Ile, Gly and Ser, whereas in *Pf*LDH it interacts with Phe and Asn (**Figure 5**).

Table 3 The binding affinity value of *Pf*DHODH and *Pf*LDH.

Compound	Binding affinity (kcal/mol)	
	***Pf*DHODH**	***Pf*LDH**
(1)	−9.94 ± 0.11	−8.84 ± 0.11
Chloroquine	−6.83 ± 0.08	−7.44 ± 0.06
Native ligand (inhibitor)	−13.95 ± 0.12	−13.02 ± 0.01

Coumarin compounds show an inhibiting effect on η-class carbonic anhydrase, thereby affecting the mediation of proton extrusion and the transport of acid/base equivalents, including bicarbonate and lactate, across the cell membrane [21,22]. The inhibition of η-class carbonic anhydrase influences ATP requirements in malaria parasites by facilitating the conversion of pyruvate to lactate through the action of lactate dehydrogenase [23]. Coumarin compounds are recognized for their activity on *Pf*DHODH, which functions in mitochondria [24]. This approach indicates that compound (1) has a mechanism of action on *Pf*DHODH and *Pf*LDH.

Molecular modeling is an effective technique that enables the short-term prediction of a variety of noteworthy compounds. In medicinal chemistry, *in silico* applications can assess the pharmacological properties and receptor interactions of lead compounds [25]. To predict the affinity and binding mode of ligands within their binding domains, molecular docking has been extensively employed [26]. *Pf*DHODH and *Pf*LDH proteins are employed as macromolecules for this aim due to the chemical similarity in ligand co-crystals to compound (1). Amino acid binding in the *Pf*DHODH co-crystal is predominantly observed in the aromatic, ketone, amide and hydroxyl structures, which exhibit a strong affinity for the hydrogen bond. Conversely, in *Pf*LDH, the hydroxyl, ketone and amide structures are particularly essential for binding the hydrogen bond (**Figure 5**). Amino acids in compound (1) have similar H-bond binding interactions with the *Pf*DHODH protein at specific sites: Ile508, Gly507, Gly478 and Ser477. These interactions are involved in binding ketone and hydroxyl groups (**Figure 6(A)**). The *Pf*LDH protein correlates with the co-crystal, specifically at the Phe100 residue that is attached to the ketone group (**Figure 6(B)**).

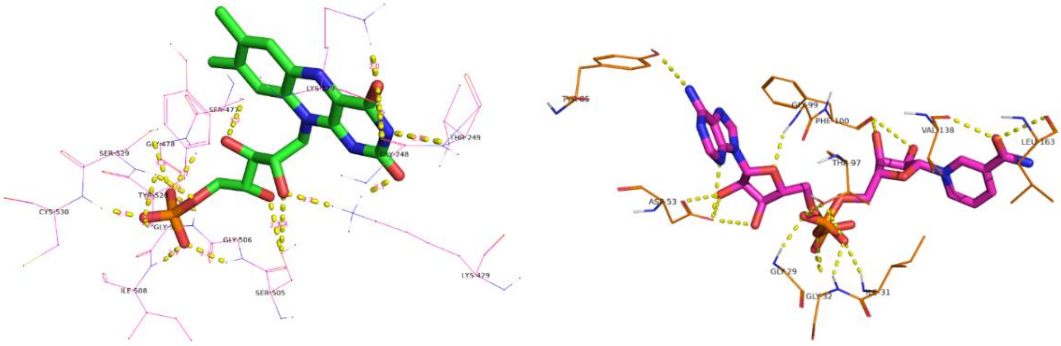

Figure 5 Visualization of interaction *Pf*DHODH and *Pf*LDH with co-crystal FMN and NAI, respectively.

In chloroquine, there are only 2 amino acids that involve hydrogen bonds, which are similar to those found in the co-crystal ligand (**Figures 6(C)** and **6(D)**). It is the factor that leads to the superior binding affinity of compound (1) compared to chloroquine. Furthermore, chloroquine is recognized for its action

within the food vacuole, where *Plasmodium* metabolizes hemoglobin releasing the toxic monomeric α-hematin (ferriprotoporphyrin IX) as a by-product. The parasites, lacking the heme oxygenase pathway, depend on a distinct α-hematin sequestration mechanism to synthesize hemozoin. Consequently, chloroquine obstructs the conversion of heme into hemozoin crystals, thereby compromising the survival of *Plasmodium* [27-29].

.

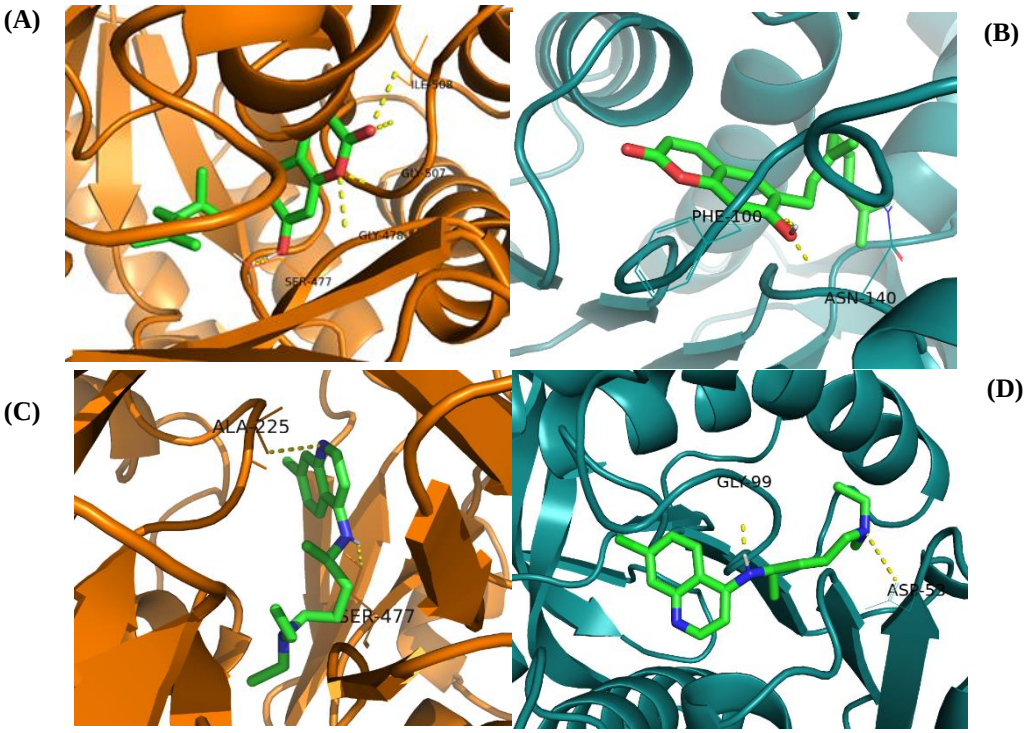

Figure 6 Interaction of compounds at various active sites in the *P. falciparum*. Interaction of Compound (1) and chloroquine against *Pf*DHODH (A, C) and *Pf*LDH (B, D).

Toxicity prediction

Toxicity evaluation is important to ensure that drug candidates are safe. Protox-III provides toxicity prediction accuracy > 85 % [19]. Prediction is done by looking at organ toxicity and toxicity endpoints such as hepatoxicity, carcinogenicity, immunotoxicity, mutagenicity and cytotoxicity (**Figure 7**). The risk of toxicity of the compounds ostruthin by looking at the 3 toxic descriptors mutagenicity, hepatotoxic and LD_{50} as the main components of the assumption. Ostruthin does not provide mutagenic properties in triggering genetics or DNA. Hepatotoxicity is an important cause of drug withdrawals; unfortunately, 1-quarter of marketed pharmaceuticals are retracted due to adverse hepatic effects, and ostruthin is not toxic to the liver effects (**Figure 7**). Assessing acute toxicity is a crucial aspect of drug discovery and development. Acute toxicity is represented by the lethal dose value (LD_{50}), which denotes the quantity of the test compound that resulted in the mortality of 50 % of the treated animals within a specified timeframe. LD_{50} value of the ostruthin showed a non-toxic effect compared to chloroquine.

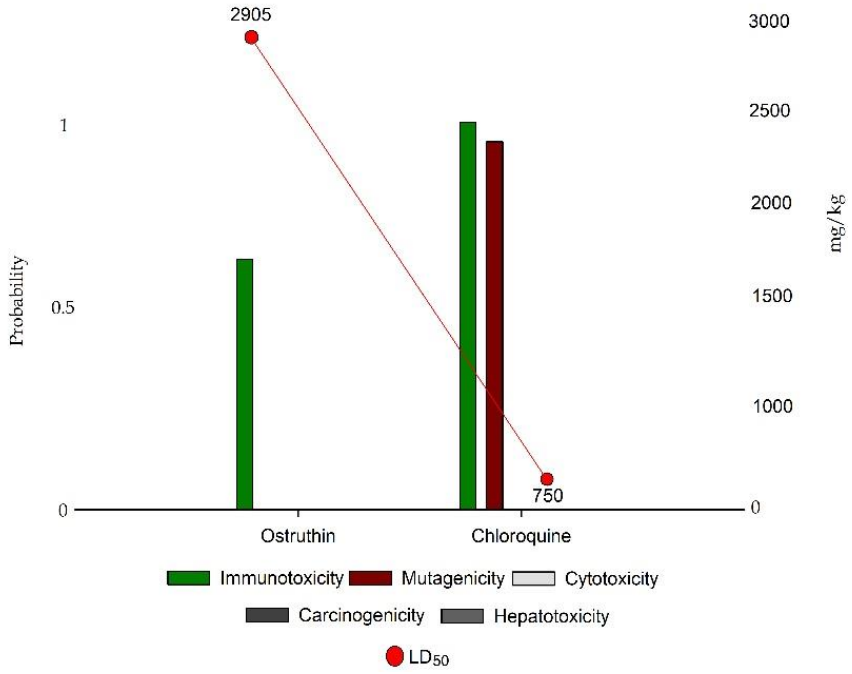

Figure 7 Toxicity parameters' prediction with Protox-II. The predicted LD_{50} value of Ostruthin (2,905 mg/kg) was encountered in class 5 of GHS, being high than chloroquine (750 mg/kg) in class IV.

Conclusions

Ostruthin isolated from the root and stem of *L. sarmentosa* is active as an antimalarial. This compound is interesting for further developing new antimalarial agents, especially in the mechanism of action of *Pf*DHODH and *Pf*LDH inhibition. However, further *in vivo* research is needed to determine the antimalarial and toxicity activity of ostruthin in experimental animals.

Acknowledgements

The authors are grateful to the Ministry of Research and Technology, Republic Indonesia, for the "Penelitian Disertasi Doktor (PDD)" scheme with contract no. 1239/UN3.LPPM/PT.01.03/2023.

References

[1] World Health Organization. World malaria report 2023, Available at: https://www.who.int/teams/global-malaria-programme/reports/world-malaria-report-2023, accessed June 2024.

[2] Ministry of Health RI. *Annual malaria report 2022*. Vol. XI. Directorate General for Disease Prevention and Control, Ministry of Health RI, Jakarta, Indonesia, 2023, p. 135-139.

[3] N Mishra, RS Bharti, P Mallick, OP Singh, B Srivastava, R Rana, S Phookan, HP Gupta, P Ringwald and N Valecha. Emerging polymorphisms in falciparum Kelch 13 gene in Northeastern region of India. *Malaria Journal* 2016; **15**, 583.

[4] D Tungmunnithum, A Thongboonyou, A Pholboon and A Yangsabai. Flavonoids and other phenolic compounds from medicinal plants for pharmaceutical and medical aspects: An overview. *Medicines* 2018; **5(3)**, 93.

[5] K Karunamoorthi and E Tsehaye. Ethnomedicinal knowledge, belief and self-reported practice of local inhabitants on traditional antimalarial plants and phytotherapy. *Journal of Ethnopharmacology* 2012; **141(1)**, p. 143-150.

[6] P Sirinut, A Petchkongkeaw, J Romsaiyud, S Prateeptongkum and P Thongyoo. Phytochemical constituents from the root of *Luvunga scandens* and biological activity evaluation. *Natural Product Communications* 2017; **12(9)**, 1483-1484.

[7] W Ahmad, H Ilmi, L Tumewu, DK Sari, AF Hafid and A Widyawaruyanti. *Luvunga scandens* (Roxb)

as the promising source of antimalarial drugs against *Plasmodium falciparum* 3D7. *Journal of Research in Pharmacy* 2024; **28(3)**, 891-898.

[8] S Syarpin, S Permatasari and D Pujianto. Analysis of phytochemical constituents and antioxidant activity from the fractions of *Luvunga sarmentosa* root extract using LCMS/MS. *Biodiversitas* 2023; **24(2)**, 733-740.

[9] AF Hafid, H Ilmi, U Islamiati, HK Nisa, L Tumewu, M Adianti, TS Wahyuni, S Suciati and A Widyawaruyanti. The combination of *Luvunga sarmentosa* (BI.) and *Eurycoma longifolia* Jackhydro-alcoholic extract as a source of antioxidant and analgesic agent. *Journal of Research in Pharmacy* 2023; **27(2)**, 642-651.

[10] A Hafizi, A Rahmadi, D Diana, U Progaram and S Kehutanan. Etnobotani tanaman obat oleh masyarakat dayak meratus di Kecamatan Halong Kabupaten Balangan Provinsi Kalimantan selatan (*in Indonesian*). *Jurnal Sylva Scienteae* 2022; **5(1)**, 8-13.

[11] N Wathan, R Rina, N Rahmah, H Aulia and N Pujianti. Etnobotani tumbuhan obat oleh etnis dayak meratus di desa gunung riut kabupaten balangan kalimantan selatan (*in Indonesian*). *Pharma Xplore: Jurnal Sains dan Ilmu Farmasi* 2023; **8(1)**, 35-48.

[12] MA Rashid, AI Gray, PG Waterman and JA Armstrong. Novel C-geranyl 7-hydroxycoumarins from the aerial parts of *Eriostemon tomentellus*. *Zeitschrift für Naturforschung B* 1992; **47(2)**, 284-287.

[13] C Lambros and JP Vanderberg. Synchronization *of Plasmodium falciparum* erythrocytic stages in culture. *The Journal of parasitology* 1979; **65(3)**, 418-420.

[14] X Wang, Y Miyazaki, DK Inaoka, ED Hartuti, YI Watanabe, T Shiba, S Harada, H Saimoto, JN Burrows, FJG Benito, T Nozaki and K Kita. Identification of *Plasmodium falciparum* mitochondrial malate: Quinone oxidoreductase inhibitors from the pathogen box. *Genes* 2019; **10**, 471.

[15] LK Basco, S Mitaku, AL Skaltsounis, N Ravelomanantsoa, F Tillequin, M Koch and J Le Bras. *In vitro* activities of furoquinoline and acridone alkaloids against *Plasmodium falciparum*. 1994; **38(5)**, 1169-1171.

[16] MF Dolabela. *In vitro* antiplasmodial activity of extract and constituents from *Esenbeckia febrifuga*, a plant traditionally used to treat malaria in the Brazilian Amazon. *Phytomedicine* 2008; **15(5)**, 367-372.

[17] R Batista, AJS Júnior and AB De Oliveira. Plant-derived antimalarial agents: New leads and efficient phytomedicines. Part II. Non-alkaloidal natural products. *Molecules* 2009; **14(8)**, 3037-3072.

[18] YT Liu, Y Ju and XM Qin. Studies on the compatibility mechanism and material basis of Danggui Buxue Decoction against anemia mice using metabonomics and network pharmacology. *Journal of Pharmacy and Pharmacology* 2021; **73(6)**, 767-777.

[19] P Banerjee, AO Eckert, AK Schrey and R Preissner. ProTox-II: A webserver for the prediction of toxicity of chemicals. *Nucleic Acids Research* 2018; **46(W1)**, W257-W263.

[20] K Kang, WDC Schenkeveld, G Weber and SM Kraemer. Stability of coumarins and determination of the net iron oxidation state of iron-coumarin complexes: Implications for examining plant iron acquisition mechanisms. *ACS Earth and Space Chemistry* 2023; **7(12)**, 2339-2352.

[21] HM Becker. Carbonic anhydrase IX and acid transport in cancer. *British Journal of Cancer* 2022; **122(2)**, 157-167.

[22] S Giovannuzzi, V De Luca, A Nocentini, C Capasso and CT Supuran. Coumarins inhibit η-class carbonic anhydrase from *Plasmodium falciparum. Journal of Enzyme Inhibition and Medicinal Chemistry* 2022; **37(1)**, 680-685.

[23] M Jakubowski, E Szahidewicz-Krupska and A Doroszko. The human carbonic anhydrase II in platelets: An underestimated field of its activity. *BioMed Research International* 2018; **2018(1)**, 4548353.

[24] N Irfan, P Vaithyanathan, H Anandaram, SM Zaidh, SP Varshini and A Puratchikody. Active and allosteric site binding MM-QM studies of *Methylidene tetracyclo* derivative in PCSK9 protein intended to make a safe antilipidemic

agent. *Journal of Biomolecular Structure and Dynamics* 2023; **42(13)**, 9-14.

[25] RK Goel, D Singh, A Lagunin and V Poroikov. PASS-assisted exploration of new therapeutic potential of natural products. *Medicinal Chemistry Research* 2011; **20(9)**, 1509-1514.

[26] P Ravula, HB Vamaraju, M Paturi, NSC Jn and S Kolli. Design, synthesis, *in silico* toxicity prediction, molecular docking, and evaluation of novel pyrazole derivatives as potential antiproliferative agents. *EXCLI Journal* 2016; **15**, 187-202.

[27] PTV Nguyen, GLT Nguyen, OT Đinh, CQ Duong, LH Nguyen and TN Truong. In search of suitable protein targets for anti-malarial and anti-dengue drug discovery. *Journal of Molecular Structure* 2022; **1256**, 132520.

[28] E Hempelmann. Hemozoin biocrystallization in *Plasmodium falciparum* and the antimalarial activity of crystallization inhibitors. *Parasitology Research* 2007; **100(4)**, 671-676.

[29] AP Gorka, A De Dios and PD Roepe. Quinoline drug-heme interactions and implications for antimalarial cytostatic versus cytocidal activities. *Journal of Medicinal Chemistry* 2013; **56(13)**, 5231-5246.